Master Thesis

Rate-induced critical transitions in tidal marsh ecosystems

Floris Neijnens
4110099

A creek cross-cutting a vegetated salt marsh plain in
Het Verdronken Land van Saeftinghe*, Zeeuws-Vlaanderen*

Degree: Sustainable Development, track Environmental Change and Ecosystems
Supervisors: dr. Koen Siteur, prof. dr. ir. Max Rietkerk, prof. dr. Rob de Boer
Date of submission: 2nd of August, 2019

Abstract

Salt marshes are important coastal ecosystems because of their function as coastal protection and their ecological relevance. Many salt marshes in the world are threatened by an increasing rate of sea level rise. Because of a positive feedback loop between sedimentation and vegetation growth, salt marshes can exhibit a rate-induced critical transition induced by sea level rise. However, a general framework for analysing salt marsh collapse in terms of creek patterns and vegetation productivity is still lacking. In this thesis, a spatial and a non-spatial salt marsh model are analysed in terms of ecosystem stability and the presence of rate-induced early warning signals. This research shows a higher suspended sediment concentration and growth of plants which are better at capturing sediment increases salt marsh stability for high rates of sea level rise. Furthermore, it is concluded spatial processes do not have an influence on the rate of sea level rise at which the rate-induced critical transition occurs. Lastly, several early warning signals are identified for salt marsh collapse, most notably an increase in auto-correlation and variance, as well as a decrease in creek edge steepness and total salt marsh area. A better understanding of the factors influencing salt marsh stability and ecosystem behaviour close to its tipping point can help policy makers to better assess vulnerability of salt marshes around the world and identify potential measurements to protect these ecosystems.

Keywords: Salt marsh dynamics, sea level rise, spatial pattern formation, rate-induced critical transitions, early warning signals.

Table of contents

Introduction

Salt marshes are important ecosystems which form in the intertidal coastal zone (Morris et al., 2013). A variety of plants can grow in salt marshes, which are able to cope both with the stress of salt as well as the partial inundation of the marsh due to tidal forcing. Salt marsh vegetation forms elaborate spatial patterns with alternating vegetation patches entrenched by creeks through which seawater can flow (Bertness and Ellison, 1987). Currently, anthropogenic factors put increasing stress on salt marshes, including pollution and their exposure to high rates of relative sea-level rise (Kirwan and Megonigal, 2013). Relative sea-level is expected to increase for most parts of the world, and this will lead to increased inundation of salt marshes (Roman, 2017).

Sustainability issue

Salt marshes are interesting ecosystems to study, both from a societal and a scientific perspective. From a societal perspective, wetlands can function as coastal protection structures, as well as improve water quality, food provision and recreational opportunities (Meire et al., 2005; Morris et al., 2013). The vegetation in salt marshes can function as a coastal protection structure, because of their ability to attenuate waves (Reed et al., 2018). For storms, modelling studies also indicate that tidal ecosystems can function as 'soft coastal protection' (van Maanen et al., 2015). This natural barrier will then act as a protector for hard coastal protection (e.g. dikes) which are further landwards.

Salt marshes are also relevant to study from a scientific point of view. Currently, salt marshes are exposed to high levels of relative sea-level rise; these rates will increase further in the following decades. Because of the positive feedback between plant growth and sediment accumulation, it is expected that salt marshes undergo a tipping point if sea level rise exceeds a certain threshold (van de Koppel et al., 2005; Kirwan and Guntenspergen, 2010). However, a general framework for analysing these transitions is still lacking. Furthermore, salt marshes show distinct patterning caused by growing vegetation on the marsh, combined with creeks which transport water and sediment through the system. This patterning is considerably different from patterns which are observed in other ecosystems, such as arid vegetation patterns (Rietkerk et al., 2004). Better understanding how patterns change if salt marshes are exposed to stress factors such as increased inundations, can help to determine possible early warning signals which indicate the salt marsh is close to collapse.

Salt marsh stability

The stability of tidal marsh ecosystems is dependent on how these systems are formed and how they can grow and retreat. Saltmarsh establishment occurs via the random dispersal of seeds in the near-coast sediment. For colonization to succeed, a threshold sedimentation rate and low wave energy are required, for which the threshold conditions differ among plant species (Willemsen et al., 2018). Once established, the plant grows via the lateral expansion of its roots to form a patch (Reed et al., 2018). Vegetation establishment causes sedimentation to increase in the patch, because of the ability of plants to decrease water flow. Sedimentation will in turn decrease the inundation time of the plant, which will lead to increased biomass productivity. Vegetation growth will also lead to an increased water flow in the interpatch area, thereby increasing erosion and causing creeks to form between patches of vegetation. Eventually, these processes will lead to the characteristic patterns which are observed in salt marsh vegetation (Bertness and Ellison, 1987).

Many ecosystems exhibit critical transitions, meaning a change in an environmental condition will cause a sudden change of the ecosystem state (Scheffer et al., 2001). Usually, an ecosystem moves towards a degraded state after a critical transition, for example the collapse of vegetation growth in dryland ecosystems when rainfall decreases (Rietkerk et al., 2004). When analysing critical transitions in ecological models, a steady state analysis is applied to determine the change in a parameter needed to switch an ecosystem to an alternative stable state. However, steady state analysis assumes that the ecosystem is constantly in a dynamic equilibrium. It can be argued that this is not always the case, especially in the current Anthropocene era in which fast environmental changes are observed (Rockström et al., 2009). Therefore, the concept of rate-induced critical transitions has been proposed (Scheffer et al., 2008; Siteur et al., 2016). This concept is different from a classical critical transition because it is not assumed that the system is in a dynamic equilibrium, but instead external conditions are constantly changing. Ecosystems which exhibit a critical transition often also display early-warning signals, which are statistical characteristics of the system when close to such a critical transition (Scheffer et al, 2009). Just as regular critical transitions, rate-induced critical transitions can also exhibit early warning signals which signal proximity to a bifurcation point (Siteur et al., 2016; Ritchie and Sieber, 2018).

In salt marshes, it is the rate of sea level rise which has an influence on ecosystem stability, as opposed to the sea level itself. If sea level rise is above a certain threshold value, the vegetation will inundate and therefore the salt marsh will die off. This is an example of a rate-induced critical transition, where the rate of change of a system parameter will cause a catastrophic shift of the ecosystem state (Siteur et al., 2016). Several modelling studies have looked at the influence of sea-level rise on salt marsh stability. Morris et al. (2002) focus on the deposition of sediment on the marsh, which is facilitated by vegetation which captures sediment particles. If relative sea level rise is above a certain threshold level, the saltmarsh vegetation will not be able to capture enough sediment and will over time submerge.

Besides internal marsh dynamics, salt marsh stability also depends on the stability of the cliff edge of the salt marsh. At the cliff edge, there are cyclic alternations between salt marsh expansion and retreat (Bouma et al., 2016). Saltmarsh expansion requires a favourable environment for seedling establishment, as discussed above. Saltmarsh retreat occurs by erosion of the saltmarsh edge, which is usually characterised by a cliff edge. Bouma et al. (2016) indicate that erosion occurs if short-term sediment dynamics on the adjacent mudflat are high and the elevation above mean sea level is low. In addition, the modelling study by van de Koppel et al. (2005) indicates that the patterns in salt marshes, created by a positive feedback between plant growth and sedimentation, increase the height of the cliff with the mudflat, which leads to a higher instability of the ecosystem.

Salt marsh patterning

Regarding the formation of spatial patterns in tidal marshes, several mechanisms have been put forward looking at the internal dynamics of a salt marsh. Classically, pattern formation was explained by scale-dependent feedback, which causes local activation and long-range inhibition of a substance, as originally proposed by Turing (1952). An example of this type of patterning is the formation of vegetation patches in precipitation-depleted drylands (Rietkerk et al., 2002). The vegetation patterning in these ecosystems can change close to a critical transition and can therefore serve as an early warning signal for ecosystem collapse (Rietkerk et al., 2004). Another mechanism regarding pattern formation is the aggregation of species at places where there is a higher density, according to the phase separation principle (Liu et al., 2013). Aggregation patterns occur in many different systems, e.g. mussel clumping or corpses of ants (Liu et al., 2016), as well as in seagrass meadows due to waterfowl predation (van der Heide et al., 2012).

Patterns in salt marshes form because of the alternation between vegetated patch areas and channels of water, which form either because of river water (in a delta) or because of tidal forces (in a salt marsh). Several methods have been applied to model salt marsh dynamics, not using either a Turing mechanism or aggregation patterns (see e.g. Morris et al., 2002; Kirwan et al., 2010). Instead, these studies explain the stability of salt marshes using sediment dynamics and vegetation productivity. Kirwan and Murray (2007) describe a spatially explicit model which describes saltmarsh development over time, taking into account deposition and erosion of sediment, as well as diffusion of sediment through the saltmarsh, depending on the presence of vegetation. It is concluded that a higher tidal range will increase sediment accretion in the vegetated areas, which will in turn increase the stability of the salt marsh with rising sea level. Overall, these studies show that modelling can increase the understanding of salt marsh stability and unravelling which factors have an impact of the resilience of the system.

Problem definition

Much is known about the establishment of vegetation on the tidal mudflat before the salt marsh. Besides this, many studies have looked at the stability of the edge of the salt marsh, and the cyclicity of the protruding and eroding phase (Bouma et al., 2016; van de Koppel et al., 2005). However, the stability of salt marshes also depends on the spatial arrangement of vegetation on the salt marsh itself, and a general framework to describe and analyse salt marsh stability under a rising relative sea level is still absent. Furthermore, salt marsh instability may also depend on other factors, e.g. the type of vegetation growing on the marsh and the amount of sediment in sea water. These factors are known to vary significantly for different salt marshes, as well on the salt marsh itself (Syvitski et al., 2005; Zedler et al., 1999) It has been illustrated in modelling studies that an increase in sea level rise will cause salt marsh vegetation to disappear (Morris et al., 2002). However, what is not clear yet is whether spatial patterning in salt marshes makes these systems more stable against sea level rise. Besides this, it is not known whether early warning signals exist for salt marsh ecosystems which are rate-sensitive. These early warning signals may not be similar to early warning signals for classical critical transitions (i.e. an increase in recovery time, variance and autocorrelation (Scheffer et al., 2009)) or to early warning signals in dryland ecosystems (Rietkerk et al., 2004).

To study the effects of relative sea level rise on salt marsh dynamics, three research questions have been formulated. The first research question is: How do vegetation productivity, suspended sediment concentration and the ability of vegetation to capture sediment affect the stability of salt-marshes subject to sea level rise? These conditions can vary locally and can therefore lead to changes in stability of salt marshes around the world. It is hypothesised that the suspended sediment concentration and the ability to trap sediment by vegetation both increase the salt marsh stability, because increased sedimentation will lead to a faster increase in salt marsh height. A higher vegetation productivity will also lead to increased sedimentation, and therefore is also hypothesised to lead to higher ecosystem stability. To answer this research question, a non-spatial mathematical salt marsh model will be used. A sensitivity analysis will be performed to determine the effect of a changing parameter on the salt marsh stability.

The second research question is: How do spatial processes affect the critical rate of sea level rise above which sedimentation in salt marsh ecosystems cannot keep up with sea level rise? It is hypothesised that spatial processes, such as sediment diffusion and channel formation, make the system more stable against sea level rise. Modelling studies have shown that pattern formation has a stabilizing effect in arid ecosystems with low rainfall (Rietkerk et al., 2002). A modelling approach will be used to answer this question, which makes it possible to compare a spatial and a non-spatial model of salt marshes. This allows to determine the effect spatiality has on salt marsh dynamics when exposed to sea level rise.

The third research question is: How can the proximity to a rate-induced critical transition in salt marshes be inferred from statistics on time series and/or spatial patterns? It is hypothesised that a rate-induced critical transition in salt marshes shows similar early warning signals as described by Scheffer et al. (2009) for classical critical transitions, i.e. an increase in the half-time, the auto-correlation and the variance. Besides this, it is expected that spatial early warning signals are present which are specific for salt marsh ecosystems. Close to the rate-induced transition, the hypothesis is that the total salt marsh area is decreased and that the creek edge becomes less steep, because a too high inundation stress causes no vegetation to grow in the creeks. To answer this research question, both models which were used for the first and second research question will be analysed for different rates of sea level rise.

Theoretical framework

Non-spatial 'Morris-model'

The non-spatial model describing salt marsh development which is used in this study will be based on Morris et al. (2002) and is slightly adapted by using the parameterization of the study by Kirwan and Guntenspergen (2007). The model consists of a set of three ordinary differential equations. These equations describe the development of the saltmarsh height (*Y2*), the mean high tide (*Y3*) and mean sea level (*Y1*) (see figure 1). The rate of change in mean sea level and high tide (*Y3* and *Y1*) depends on the sea level rise. The rate of change of the marsh platform depends on the depth of the marsh below the mean high tide, as well as the amount of biomass. This can be summarized in the following equations:

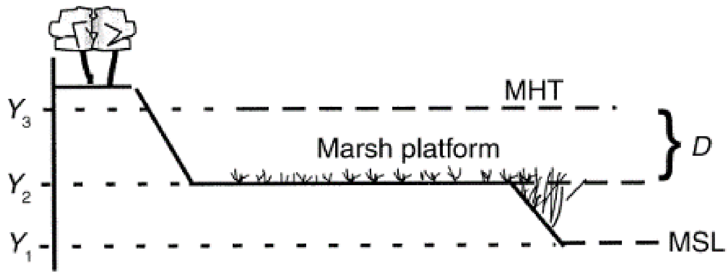

Figure 1: The depiction of mean high tide (Y3), the saltmarsh height (Y2) and the mean sea level (Y1) relative to each other (Morris et al., 2002). The depth D *is given by* D = Y3 - Y2.

$$\frac{dY1}{dt} = \frac{dY3}{dt} = r \tag{1}$$

$$\frac{dY2}{dt} = (qC_{ss} + kB)D \tag{2}$$

In which *r* is relative sea level rise in mm y^{-1}, C_{ss} is the amount of suspended sediment above the marsh platform in g m^{-3}, *q* is a proportionality constant in m^3 g^{-1} y^{-1}, and *k* represents the amount of sediment trapping by vegetation in m^2 g^{-1}. Furthermore, *B* is the biomass productivity in g m^{-2} y^{-1} and *D* is the depth of the salt marsh below mean high tide in cm, calculated by *D* = *Y3* – *Y2*. In equation (2), the biomass *B* is a parameter which is dependent on the depth *D* of the salt marsh, according to the following equation:

$$B = aD + bD^2 + c \tag{3}$$

In which *a*, *b* and *c* are scaling parameters with units g m^{-3} y^{-1} for *a*, g m^{-4} y^{-1} for *b* and g m^{-2} y^{-1} for *c*. The equation for the saltmarsh height *Y2* can now be rewritten into its final form:

$$\frac{dY2}{dt} = \left(qC_{ss} + k(aD + bD^2 + c)\right)D = kbD^3 + kaD^2 + (qC_{ss} + kc)D \tag{4}$$

Several basic assumptions are made in this model. Firstly, it is assumed that the marsh surface is stable during low tide, whereas the marsh surface will rise when the marsh is inundated; it is assumed that the rate of surface increase is proportional to the inundation time (and therefore depth below high tide). Furthermore, vegetation traps sediment, and it is assumed that vegetation density linearly increases the sedimentation rate. Note that this is an additional sedimentation flux, besides the sedimentation rate dependent on depth below high tide, which is dependent on suspended sediment in the water column (see equation 2). Vegetation can grow in the model, but this vegetation growth depends on the depth of the salt marsh. Vegetation has an optimal growing depth, as defined in equation 4, and therefore vegetation should not be constantly inundated, nor be too high above the tide. If these conditions are implemented in the model, it turns out that there is an optimal amount of sea level rise, at which marsh productivity is maximal and higher compared to vegetation productivity at a constant sea level (i.e. r = 0 mm y^{-1}).

The equations 1 and 2 can be merged into one differential equation by describing the marsh height as the depth of the marsh below mean high tide, i.e. $D = Y3 - Y2$. This gives the new equation:

$$\frac{dD}{dt} = \frac{d(Y3 - Y2)}{dt} = r - (qC_{ss} + kB)D = r - kbD^3 - kaD^2 - (qC_{ss} + kc)D \tag{5}$$

If this equation is set to zero, the rate of sea level rise r can be calculated for each value of the equilibrium depth of the salt marsh D:

$$\frac{dD}{dt} = r - kbD^3 - kaD^2 - (qC_{ss} + kc)D = 0$$

$$r = kbD^3 + kaD^2 + (qC_{ss} + kc)D \tag{6}$$

For this function, the steady states cannot be calculated analytically because this would produce a cubic equation which cannot be solved. What can be calculated is the critical depth, i.e. the depth at which the critical transition will occur and the salt marsh will be submerged. The critical depth $D_{c\,1,2}$ is then calculated by determining dr/dD and setting this equation to zero:

$$\frac{dr}{dD} = 3kbD^2 + 2kaD + qC_{ss} + kc = 0$$

$$D_{c\ 1,2} = \frac{-ka \pm \sqrt{(ka)^2 - 3kb(qC_{ss} + kc)}}{3kb} \tag{7}$$

The critical rate of sea level rise r_c can be calculated by filling in the critical depth D_c in equation 6. Lastly, the eigenvalue of the model can be calculated by adding a small perturbation *D'* to equation 5. This gives the eigenvalue of the model:

$$\lambda = -3kbD^2 - 2kaD - qC_{ss} - kc \tag{8}$$

A derivation of the eigenvalue can be found in Appendix A.

Spatial 'Kirwan-model'

In Kirwan and Murray (2007), a spatially explicit partial model for salt marsh development is proposed. This model is based on the differential equations from Morris et al. (2002), with the addition of erosion, water flow, and sediment diffusion. In this thesis, a one dimensional model will be considered in which a water stream flows from the watershed to the outlet cell; a description of the full two dimensional model used by Kirwan and Guntenspergen (2007) is given in appendix B.

The model consists of one row of *n* cells which have a length *dx*, thereby modelling a transect of *x* meters. Within each cell, deposition and erosion of sediment are governed by a series of ordinary differential equations; sediment diffusion occurs every time step by redistributing the sediment driven by gravitation. Sediment deposition is described by equation 4. Sediment erosion occurs when the bed shear stress is higher than the threshold shear stress:

$$\frac{dE}{dt} = \begin{cases} m\frac{\tau_b - \tau_c}{\tau_c}, & \tau_b > \tau_c \\ 0, & \tau_b \le \tau_c \end{cases} \tag{9}$$

In which *E* is the erosion in kg m^{-2}, *m* is a scaling constant with unit kg m^{-2} s^{-1}, τ_b is the bed shear stress in N m^{-2} and τ_c is the threshold shear stress in N m^{-2}. It is assumed that erosion occurs for only 10 minutes during each tidal cycle, so the erosion rate can be calculated for each year by multiplying the erosion per tide by the number of tides per year. Furthermore, by using the sediment density ρ_s in kg m^{-3}, the erosion rate *dE/dt* can be converted to units m y^{-1} which allows it to be subtracted from the deposition rate. When calculating the erosion rate *dE/dt*, τ_c is given a fixed value, whereas τ_b varies according to the following equation:

$$\tau_b = \frac{\rho_w f_c v^2}{8} \tag{10}$$

In which ρ_w is the density of water in kg m^{-3}, f_c is a dimensionless friction parameter and *v* is the velocity of the water in m s^{-1} flowing over the marsh surface.

In order to determine the water flow over one cell, all upstream cells which transport water from the watershed to a particular cell need to be considered. During each tidal cycle, the area will inundate to mean high tide level, after which the water will retreat again. The total amount of water flowing over a cell therefore is the cumulative sum of the water depth at high tide on the considered cell as well as the water depth of all cells upstream of the considered cell. In mathematical terms, this implies:

$$V = \int_w^x [Y1 - Y2(x)]dx = \int_w^x D(x)dx \tag{11}$$

In which *V* is the total water volume flowing perpendicular to the flow direction in m^2, *x* is the distance of the cell from the water divide in metres, and *w* is the water divide (implying *x* = 0 m). The volume *V* for each cell is divided by 3 h, the time in which the reflux of the tidal water to the sea occurs. Furthermore, for each cell *V* is divided by the high-tide water depth *D*, so water flow is higher in shallower areas compared to deeper areas. This water flow *v* is used in equation 10 to calculate the erosion rate.

In order to avoid too large differences in saltmarsh height between neighbouring cells, a sediment flux parameter is added to the model. The sediment flux depends on the slope between adjacent cells, as well as the amount of biomass productivity; a higher biomass productivity will lead to sediment stabilization and therefore to a lower diffusion factor:

$$q_s = (\alpha - \beta B)S \tag{12}$$

In which q_s is the sediment flux in m^2 y^{-1}, α the diffusion rate without vegetation growth in m^2 y^{-1}, β represents the sediment stabilization by vegetation in m^4 g^{-1}, and *S* is the slope in cm m^{-1}. The sediment flux q_s is divided by the cell length *dx* to obtain the diffusion velocity.

In both the Kirwan-model and Morris-model, a rate of sea level rise *r* is implemented to study how the system will respond to a continuously rising sea level. In the Morris-model, a rate-induced critical transition occurs when sea level rise is higher than the rate of sediment deposition. In the Kirwan-model, the salt marsh height depends on the sediment deposition, erosion and diffusion; these processes collectively determine whether a cell will become part of the salt marsh of if it will be inundated and form part of the water creek. Although the model does include spatial self-organization, no scale-dependent feedback has been implemented in this model (as discussed by Wesenbeeck et al., 2008).

Early warning signals

There are several approaches to examine how proximity to a rate-induced critical transition could be indicated by changes in the system state. If the system goes through a bifurcation, then the eigenvalue of the system will approach zero. If the eigenvalue of the system goes towards zero, then close to the bifurcation point the system will become increasingly slow in recovering from perturbations in the system (Scheffer et al., 2009; Boerlijst et al., 2013). This can be demonstrated by calculating the recovery time from perturbations, the temporal auto-correlation and the variance (Siteur et al., 2016). These are related to the eigenvalue via the following formulae:

$$t_h = \frac{1}{\lambda} ln\left(\frac{1}{2}\right) \qquad (13a)$$

$$\alpha = e^{\lambda \Delta t} \qquad (13b)$$

$$VAR = \frac{\sigma^2}{1-\alpha^2} \qquad (13c)$$

in which t_h is the half time, α is the lag-1 auto-correlation, *VAR* is the variance, Δt is the time interval with which noise is applied on the state variables, and σ is the standard deviation of the applied noise. However, if the eigenvalue of a system cannot be determined analytically, equations 13a, 13b and 13c cannot be used. Instead, the auto-correlation can then be calculated with this formula:

$$\alpha = \frac{\sum_{i=1}^{n}(a_i - \bar{a})\left(b_i - \bar{b}\right)}{\sqrt{\sum_{i=1}^{n}(a_i - \bar{a})^2 \; \sum_{i=1}^{n}\left(b_i - \bar{b}\right)^2}} \qquad (14)$$

in which n is the sample size, a_i and b_i are both values in the vectors a and b respectively, both representing the development of the considered state variable over time with b having a lag of Δt years over a. The variables $\bar{a}$ and $\bar{b}$ represent the average of the vectors a and b respectively. In the same manner, the variance is calculated using the formula:

$$VAR = \frac{1}{n}\sum_{i=1}^{n}|a_i - \bar{a}|^2 \tag{15}$$

Besides general early warning signals, salt marshes may also exhibit early warning signals which are ecosystem-specific. An important difference between salt marshes and other ecosystems is that salt marsh productivity is expected to increase near a rate-induced critical transition (Kirwan and Megonigal, 2013). This phenomenon will in turn have an influence on the spatial patterning near the critical transition (see Kéfi et al., 2014). Firstly, the cliff steepness between the salt marsh and the creek can be calculated by taking the maximum slope value, with unit cm m^{-1}. Secondly, the length of the salt marsh relative to the total length of the water flow to the outlet cell can be calculated. The salt marsh area is defined as the cells having a depth higher than the critical depth D_c (see equation 7). These properties will be further discussed in the results section.

Technical research design

Research strategy

In this study, a quantitative research strategy will be adopted, meaning the instrument used to answer the research questions (i.e. the salt marsh model) is determined in advance of the study in which all parameters are clearly defined (Verschuren et al., 2010). All data in this thesis are provided by the models which are adapted from Morris et al. (2002) and Kirwan and Murray (2007). The analysis will be performed in the programming language *Python*, version 3. *JupyterLab* is used as notebook and user interface for scripts written in *Python*.

Model implementation

The model implementation consists of rebuilding the models described by Morris et al. (2002) and Kirwan and Murray (2007). The non-spatial 'Morris-model' is slightly adapted to make it comparable with the 'Kirwan-model'. Firstly, the parameters from Kirwan and Murray (2007) have been used to analyse the model from Morris et al. (2002). Furthermore, the coefficient q has been split in two new parameters, i.e. the proportionality constant q and the suspended sediment concentration C_{ss}. The initial mean high tide is 50 cm, and the saltmarsh height is initially set at 30 cm.

The Kirwan-model is based on the Morris-model; therefore the two models can be said to have the same internal structure (except for spatiality). This implies the parameters can directly be compared with each other and no scaling of parameters needs to be applied. The spatial 'Kirwan-model' in this thesis represents a transection of 3km length through a salt marsh, with on one boundary side the water divide and on the other side the water outlet. In the model, the 3km length is represented by 600 grid cells, each having a length of 5m. The outlet cell has a predefined depth which is 500cm. The model will be initialized with the same mean high tide as in the Morris-model, and a linearly sloping salt marsh surface height from 20cm below mean high tide, until the height of the outlet cell. Both models will be run for 1000 years with a time step of 0.01 year, after which the models are assumed to be in equilibrium.

Model analysis

The model analysis consists of calculating several model properties in order to answer the three research questions as defined in the problem definition section. Firstly, a sensitivity analysis will be performed to see what the effect is of a change in parameter C_{ss}, k and c. C_{ss} represents the suspended sediment concentration in the sea water above the salt marsh, k represents the ability of plants to capture sediment and c represents the biomass productivity which is higher under more favourite climatic conditions for plant growth. These parameters will be changed within a range of -10% to +10% compared to their original value, to see what the effect is on the critical depth D_c and the critical rate of sea level rise r_c.

Several model properties are researched to determine how spatial processes affect the point at which a rate-induced critical transition occurs in salt marshes. Firstly, several model runs with different rates of sea level rise r are plotted for both the Morris-model and the Kirwan-model to show the system moves to a stable equilibrium. For the Morris-model, the biomass productivity B and the marsh depth D are plotted as a function of the rate of sea level rise r, to determine at which value of B and D the rate-induced critical transition occurs. The biomass B is then also plotted as a function of the marsh depth D. To make these plots, the model does not need to run until equilibrium for each value of r; instead, a vector with different values for marsh depth D is made, for which then the equilibrium values of r, B and the eigenvalue λ are directly calculated. The advantage for this method is that the calculated values of r, B and λ are per definition calculated for the equilibrium state, and that non-stable values for r and B (i.e. solutions to equation 5 which are not stable when running the model) can also be calculated. For the Kirwan-model, the salt marsh area is plotted as a function of the rate of sea level rise r. Salt marsh area has been defined by values in the salt marsh depth vector which are smaller than the critical salt marsh depth D_c. This salt marsh area is then divided by the total number of cells in the saltmarsh depth vector to calculate the salt marsh percentage. The model is run for 1000 years with a timestep of Δt = 0.01 year, for values of r between 0 and 10 and with Δr = 0.1. The value where the salt marsh area drops to zero percent is defined as the rate of sea level rise r where the rate-induced critical transition occurs.

For answering the third research question, several possible early warning signals are researched for a rate-induced critical transition in both the Morris-model and the Kirwan-model. For the Morris-model, the eigenvalue of the system is determined for different values of marsh depth D, biomass productivity B and the rate of sea level rise r. Furthermore, the half-time, the auto-correlation and the variance of the salt marsh depth are calculated for a range of r values between 0 and r_c (Δr = 0.1) with equations 13a, b and c.

For these calculations, it is assumed noise is added to the system with a standard deviation of $\sigma = 1$ and a time interval of 10 years. For the Kirwan-model, the variance and auto-correlation are determined for each cell in the model. However, the eigenvalue of the Kirwan-model cannot be determined analytically. Instead, additive noise with a standard deviation of $\sigma = 1$ has been added to the saltmarsh height *Y2* state variable every 10 years for the last 500 years of the model run. To compute the auto-correlation and the variance, equations 14 and 15 are used respectively. Again, the model is run for $t = 1000$ years with a timestep of $\Delta t = 0.01$ year. Lastly, two salt marsh-specific early warning signals are measured in the Kirwan-model, i.e. the cliff steepness and the salt marsh area percentage, which are plotted as a function of *r*. For the cliff steepness, the average difference with two neighbouring values is calculated for each value in the salt marsh height vector. The maximal value of this gradient vector is then plotted for each value of *r*, which then gives the cliff steepness for each value of *r*. The salt marsh area is calculated in the same manner as described in the previous paragraph.

Results

Sensitivity analysis

In this section, a sensitivity analysis has been performed on three parameters C_{ss}, k and c in the Morris-model. For this analysis, the following parameter values have been used, based on Kirwan and Murray (2007): a = 28 g m^{-3} y^{-1}, b = -0.093 g m^{-4} y^{-1}, c = -270 g m^{-2} y^{-1}, q = 0.00009 m^{3} g^{-1} y^{-1}, k = 0.000015 m^{2} g^{-1} and C_{ss} = 20 g m^{-3}. These values will used for the remainder of this section. Based on these parameter values, the salt marsh depth D_c and the rate of sea level rise r_c are calculated at which the rate-induced critical transition occurs. The critical salt marsh depth D_c is 198.0 cm and the critical rate of sea level rise r_c is 5.19 mm.

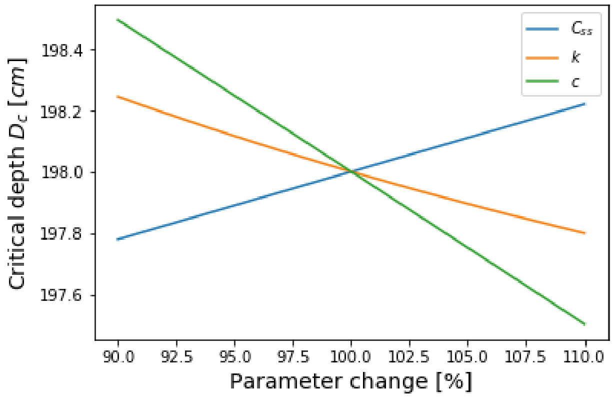

Figure 2: Sensitivity analysis for parameters C_{ss}, k *and* c *for the critical depth* D_c*. A higher suspended sediment concentration causes the critical depth to increase, whereas a higher vegetation growth and plant sediment capture leads to a lower critical depth.*

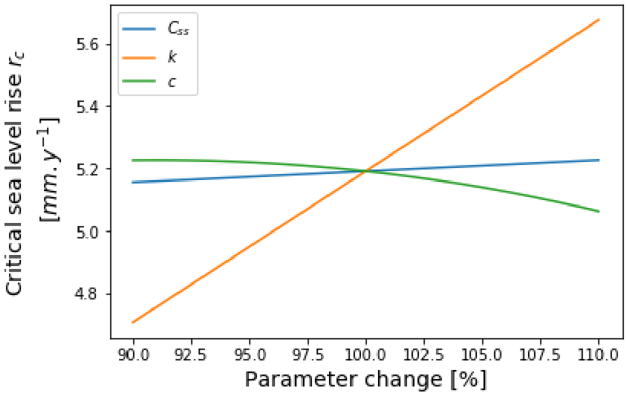

Figure 3: Sensitivity analysis for parameters C_{ss}, k *and* c *for the critical rate of sea level rise* r_c. A higher suspended sediment concentration and a higher plant sediment capture leads to a higher critical sea level rise, whereas an increase in vegetation growth leads to a lower critical sea level rise.

A sensitivity analysis has been performed for the critical depth D_c (see figure 2) and for the critical rate of sea level rise r_c (see figure 3). The critical depth will increase when there is an increase in suspended sediment concentration C_{ss} above the marsh and will decrease when plants are better able to capture sediment (parameter k) or when biomass productivity is higher (parameter c). The critical rate of sea level rise will increase with an increase in parameter k, will decrease with an increase in the parameter c and will increase slightly if there is an increase in C_{ss}. Changing the parameters C_{ss} and c has the same effect on both the critical depth and the critical rate of sea level rise, whereas increasing k leads to a lower critical depth and a higher critical sea level rise.

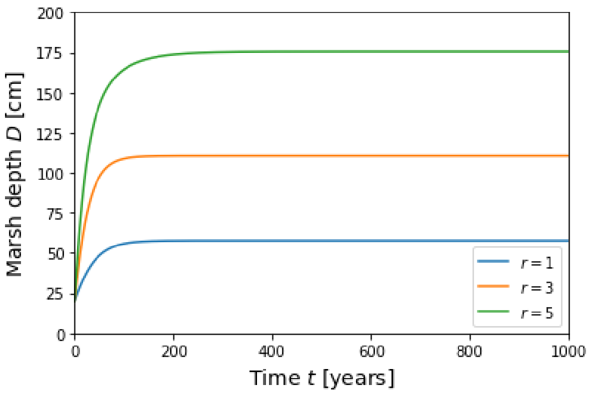

Figure 4: The development of the marsh depth D *as a function of the time* t *for* r = 1*,* r = 3 *and* r = 5*. The salt marsh depth increases with a rising rate of sea level rise.*

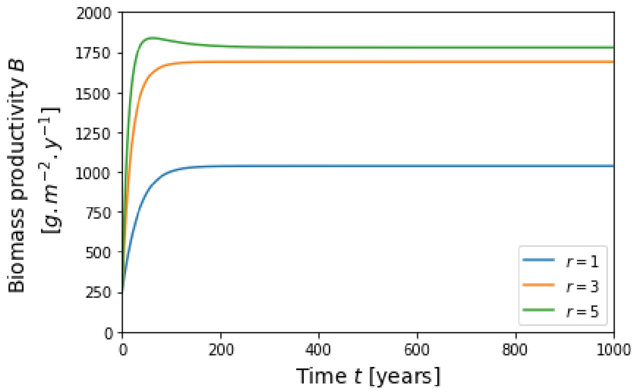

Figure 5: The development of the biomass productivity B *as a function of the time* t *for* r = 1*,* r = 3 *and* r = 5*. The biomass productivity increases with a rising rate of sea level rise.*

Effect of spatiality on rate-induced critical transitions

In this section, the point at which the critical transition occurs is compared for the non-spatial Morris-model and the spatial Kirwan-model. For the Kirwan-model, the following additional parameter values are used: m = 0.0014 kg m^{-2} s^{-1}, τ_c = 0.4 N m^{-2}, the water density is ρ_w = 997 kg m^{-3}, the sediment density is ρ_s = 450 kg m^{-3}, f_c = 0.02, α = 3.65 m y^{-1} and β = 0.0019 m^4 g^{-1}.

For the Morris-model, several model runs have been performed to confirm that the model runs will move to a stable equilibrium. In figure 4 and 5, respectively the marsh depth *D* and the biomass productivity *B* are plotted as a function of time *t* for three rates of sea level rise *r*. For all values of *r*, both the marsh depth *D* and the biomass productivity *B* are in equilibrium after ~300 years. Furthermore, a higher rate of sea level rise will lead to a higher equilibrium marsh depth. For the biomass productivity, it also seems the biomass productivity is higher if the rate of sea level rise is higher. To better determine the influence of the rate of sea level rise *r* on both the marsh depth *D* and the biomass productivity *B*, both

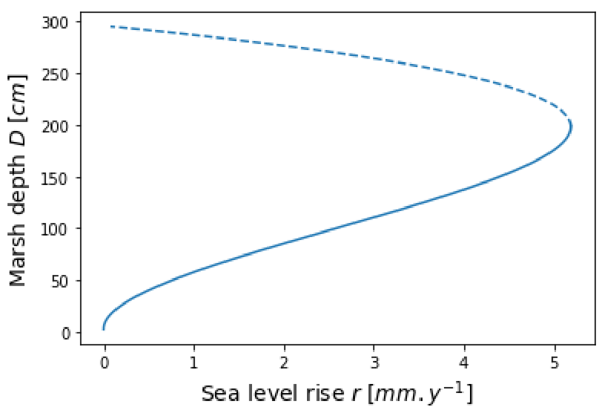

Figure 6: Marsh depth D *as a function of the rate of sea level rise* r*. Marsh depth increases with increasing sea level rise, until the rate-induced tipping point. Unstable equilibria are indicated with the dotted line.*

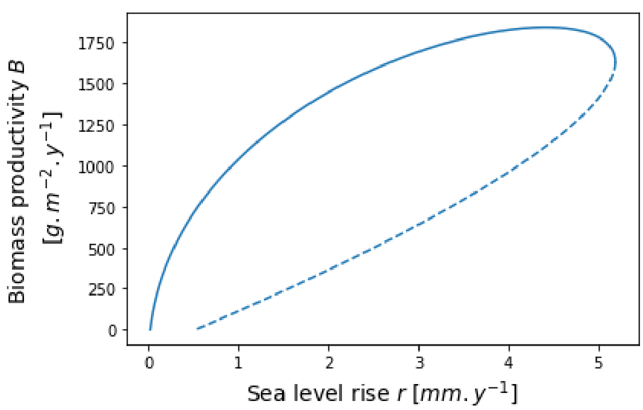

Figure 7: Biomass productivity B *as a function of the rate of sea level rise* r*. The biomass productivity shows a maximum close to the rate-induced tipping point. Unstable equilibria are indicated with the dotted line.*

these variables are plotted as a function of r (see figure 6 and figure 7). The marsh depth D increases with increasing sea level rise r, but for the biomass productivity there is a maximum value of B, after which the productivity slightly decreases towards the tipping point. At the critical marsh depth D_c, the system goes through a rate-induced critical transition and both the equilibrium depth and equilibrium biomass productivity become unstable. At this point, the critical biomass productivity B_c is 1628 g m^{-2} y^{-1} (the values for D_c and r_c are given in the *sensitivity analysis* section). Biomass productivity is at its highest at a rate of sea level rise of r_{opt} = 4.41 mm y^{-1}, which corresponds to a biomass productivity of B_{opt} = 1837 g m^{-2} y^{-1}. In figure 8, the biomass productivity B is plotted as a function of the marsh depth D, and it can be observed that the maximum value of B = B_{opt} corresponds to a value of marsh depth D_{opt} = 150.3 cm.

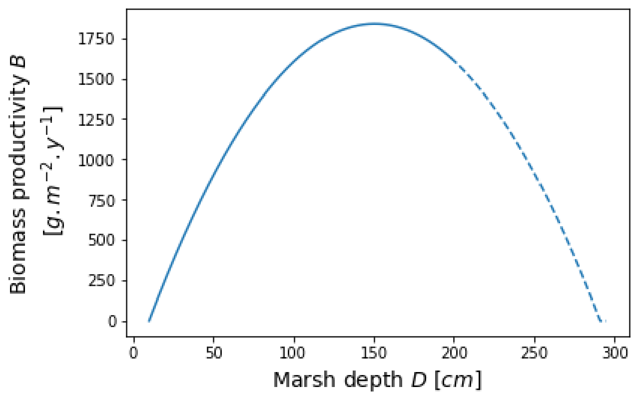

Figure 8: Biomass productivity B *as a function of the marsh depth* D. *There is an optimal stable marsh depth for which the biomass productivity is maximal. Unstable equilibria are indicated with the dotted line.*

Several model runs are also performed for the Kirwan-model, to show the difference between the spatial and non-spatial model. In figure 9, the marsh depth is depicted at t = 1000 y as a function of the distance from the water divide for three different values of r. For a higher rate of sea level rise, the marsh depth increases, as well as the depth of the water channel. Furthermore, the salt marsh length relative to the water channel length decreases with increasing sea level rise. The same trend is visible in figure 10, where the saltmarsh area is plotted as a function of the rate of sea level rise r. The saltmarsh area decreases to 0% when sea level rise is r = 5.2 mm y^{-1}. This corresponds to the value of r_c = 5.19 mm y^{-1} calculated with the Morris-model. Therefore, it can be concluded

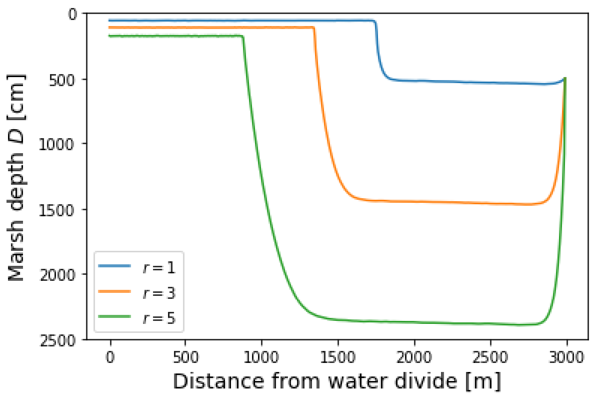

Figure 9: The marsh depth D *as a function of the distance from the water divide for* r = 1, r = 3 *and* r = 5. *Note the y-axis is reversed to indicate that a higher marsh depth corresponds to a lower salt marsh height. Both the salt marsh depth and the water channel depth increase with higher sea level rise. The marsh area relative to the total area decreases with higher sea level rise.*

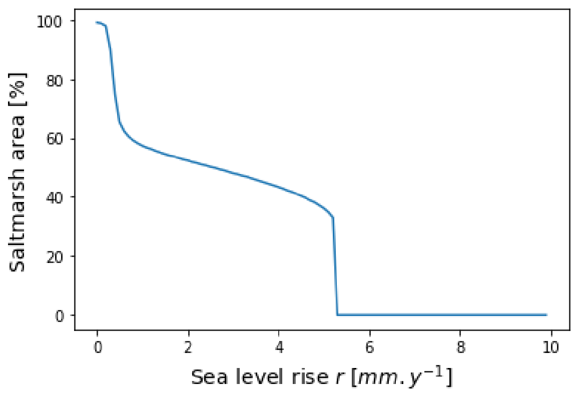

Figure 10: The salt marsh area as a function of the rate of sea level rise r. *The salt marsh area quickly decreases when* r *is slightly bigger than zero and when* r *is close to the rate-induced tipping point.*

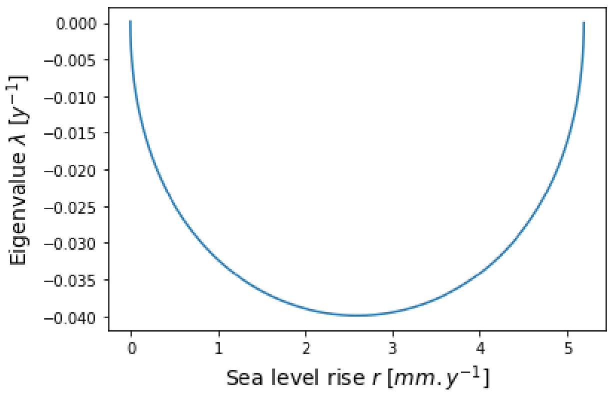

Figure 11: The eigenvalue λ *as a function of the rate of sea level rise* r. *The eigenvalue is* λ *= 0 when the rate of sea level rise r = 0 and when* $r = r_c$, *and has a minimum value of* λ *= -0.040 when the rate of sea level rise is* r *= 2.59 mm.*

that both the non-spatial and the spatial model have the same value of r_c at which the rate-induced critical transition occurs.

Early warning signals for salt marsh collapse

In this section, possible early warning signals are researched which may indicate proximity of the salt marsh system to a rate-induced critical transition. First, the stability of the Morris-model is analysed. To determine the stability for different values of the rate of sea level rise *r*, the eigenvalue can be calculated. In figure 11, the eigenvalue is plotted as a function of the rate of sea level rise *r* and in figure 12 the eigenvalue is plotted as a function of the marsh depth *D*. Both figures show a minimum in the eigenvalue for intermediate values of *r* and *D*, meaning the system is most stable at these values. In figure 13, the eigenvalue is plotted as a function of the biomass productivity *B*. This graph also shows a minimum in the eigenvalue. However, the trough of the parabola is sheared towards the

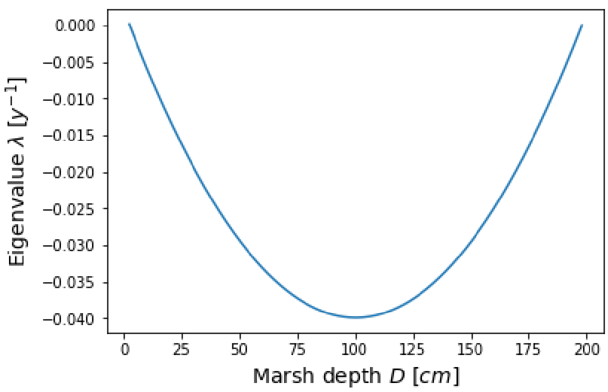

Figure 12: The eigenvalue λ *as a function of the marsh depth* D. *The minimum value of the eigenvalue corresponds to a marsh depth of* D *= 100.4 cm.*

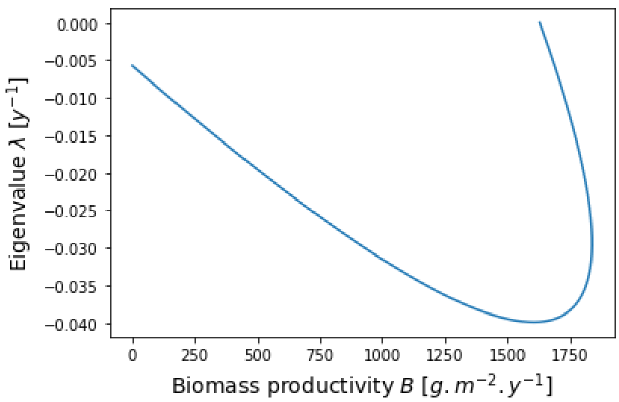

Figure 13: The eigenvalue λ *as a function of the biomass productivity* B. *The minimum value of the eigenvalue corresponds to a biomass productivity of* B *= 1603 g* m^{-2} y^{-1}. *At high values for* B, *the biomass productivity has two corresponding eigenvalues.*

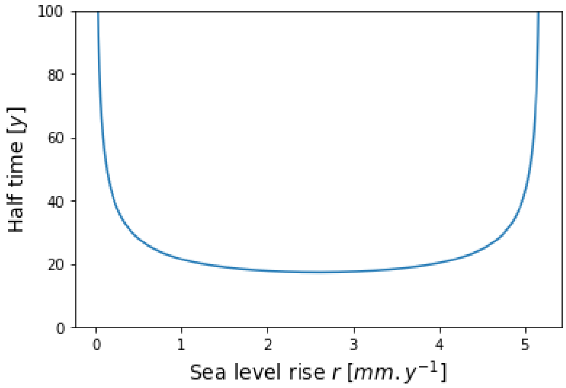

Figure 14: The half time as a function of the rate of sea level rise r *(σ = 1, Δt = 10 y). The half time has a minimum value when sea level rise is* r *= 2.59 mm and increases when approaching zero or* r_c.

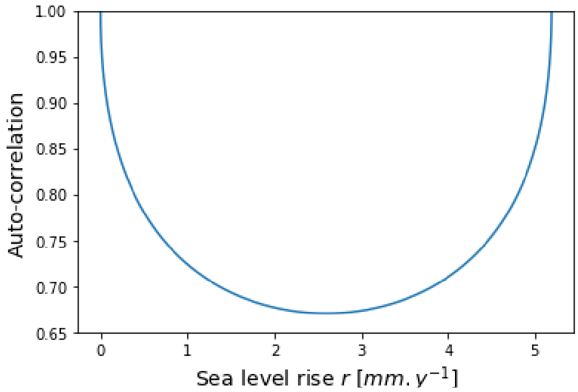

Figure 15: The auto-correlation as a function of the rate of sea level rise r *(σ = 1, Δt = 10 y). The half time has a minimum value when sea level rise is* r *= 2.59 mm and increases when approaching zero or* r_c.

right, implying the system is most stable with a high biomass productivity. Besides this, for high values of *B* there exist two values of the eigenvalue *λ* which are both stable, which in mathematical terms means *B* maps to two different values of its codomain *λ*. As a consequence, at high biomass productivity, the system can both have a very negative eigenvalue and an eigenvalue close to zero, implying biomass is not a good predictor of the stability of the system.

Three early warning signals from Scheffer et al. (2009) are tested for the Morris-model, i.e. the half-time, auto-correlation and variance (see figure 14, 15 and 16). All three early warning signals follow the same trend, which is equal to the trend of the eigenvalue in figure 11. All early warning signals have their minimum at the same value of *r* as the eigenvalue, which is *r* = 2.59 mm. When the rate of sea level rise *r* is close to *r* = 0 and to *r* = r_c, the early warning signals rapidly increase. For *r* = 0, this can be explained by noticing that both the vegetation productivity and the salt marsh depth become zero, which in turn causes the salt marsh not to be inundated anymore during floods. As a consequence,

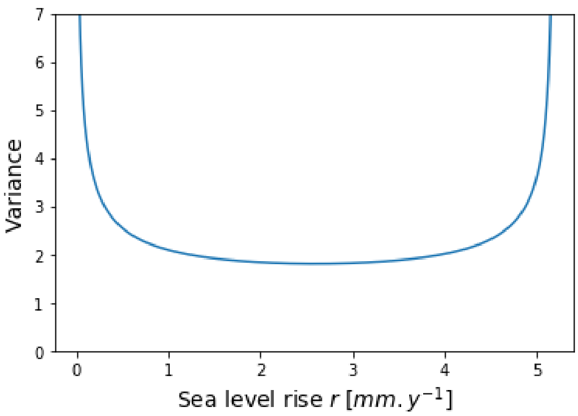

Figure 16: The variance as a function of the rate of sea level rise r *(σ = 1, Δt = 10 y). The half time has a minimum value when sea level rise is r = 2.59 mm and increases when approaching zero or* r_c.

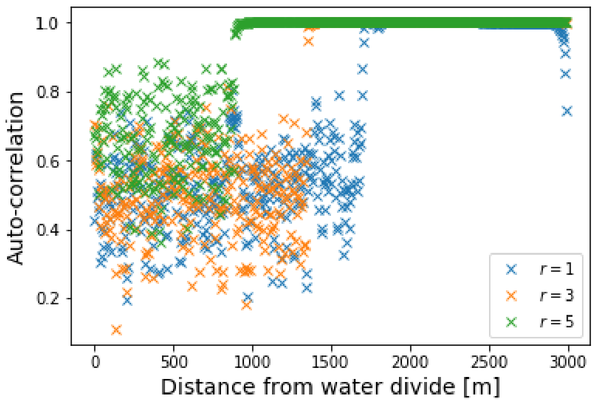

Figure 17: The auto-correlation calculated for every 5m from the water divide for r = 1, r = 3 and r = 5 (σ = 1, Δt = 10 y). The auto-correlation increases for higher values of r *on the salt marsh.*

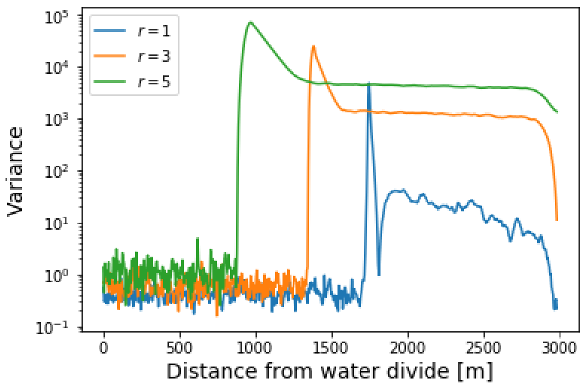

Figure 18: The variance calculated for every 5 m from the water divide for r = 1, r = 3 and r = 5 (σ = 1, Δt = 10 y). The variance is much higher in the water channel compared to the salt marsh and is highest at the cliff edge.

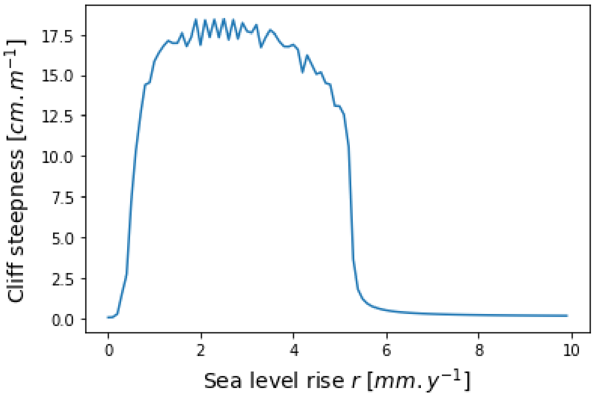

Figure 19: Cliff steepness as a function of the rate of sea level rise r*. The steepness is highest at intermediate values of* r *and decreases towards the critical sea level rise* r_c*.*

perturbations in the system cannot be restored anymore. Close to the critical transition, the marsh depth is high, implying perturbations will take a longer time to recover from the high inundation stress.

For the Kirwan-model, the auto-correlation and the variance are calculated for each cell in the salt marsh for the last 500 years of the model run. The auto-correlation and the variance are plotted as a function of the distance from the water divide (see figure 17 and 18). The auto-correlation ranges between high and low values on the marsh (i.e. between 0.2 and 0.8) and increases to 1 in the channel. Besides this, the auto-correlation on the marsh increases when the rate of sea level rise *r* is higher. Concerning the variance, the variance varies with a factor of 10 on the salt marsh. Just before the cliff, variance steeply increases, and shows a maximum at the cliff. In the water channel, the variance is much higher compared to the saltmarsh. Close to the rate-induced critical transition, the auto-correlation and variance are both considerably higher compared to lower values of *r*, and therefore can serve as useful early warning signals for salt marsh collapse.

For the Kirwan-model, two early warning signals have been researched which are specific for tidal marsh ecosystems, i.e. the creek cliff steepness and the salt marsh area relative to the total modelled area. The salt marsh area is plotted as a function of the rate of sea level rise *r* in figure 10. When *r* = 0, the salt marsh area is maximal and no water channels or creek edge is present. When *r* > 0, the salt marsh area quickly decreases, after which the decrease is less pronounced. When $r > r_c$, the salt marsh area is 0%, meaning no saltmarsh is present. The graph shows the salt marsh area is monotonically decreasing with increasing *r*, and is considerably lower close to the rate-induced tipping point. In figure 19, the cliff steepness is plotted as a function of the rate of sea level rise *r*. The cliff steepness is highest at intermediate values for r (in the range of r = 2 to r = 3) and approaches zero when the rate of sea level rise r = 0 and when $r > r_c$. When the system is approaching the rate-induced tipping point, the cliff steepness is considerably lower compared to values at intermediate sea level rise. Both the salt marsh area and the creek cliff steepness decrease when approaching the rate-induced tipping point and can therefore serve as useful early warning signals for salt marsh collapse.

Discussion

Results interpretation

To determine the effect on salt marsh stability of sediment availability, plant productivity and plant sediment trapping, a sensitivity analysis was performed on the Morris-model. This analysis showed that an increase in plant biomass productivity decreases the critical rate of sea level rise. Marsh productivity is generally higher in the tropics compared to more northern latitudes (Kirwan et al., 2009), and therefore plant productivity can be considered to increase with climate warming. These results therefore point to salt marshes becoming more prone to sea level rise in the future. However, this also depends on the ability of plants to capture sediment during flood. The analysis also showed an increase in suspended sediment concentration and the ability of vegetation to capture sediment increases the point at which the critical transition will occur. Therefore, marsh stability could possibly be increased by colonization of the marsh by new plant species which have a better ability to capture sediment. Besides this, tidal marshes which have a high sediment input are less prone to ecosystem collapse in the future. Local conditions should be taken into consideration to determine the vulnerability of salt marsh ecosystems, because the sediment concentration depends on local sea currents (Syvitski et al., 2005) and may not be uniform over the marsh surface (Zedler et al., 1999).

The effect of spatial pattern formation on the point of sea level rise at which a rate-induced critical transition would occur is researched by comparing the tipping point in the spatial and non-spatial model. The results show that a critical transition is present in both models, which causes the marsh to become unstable at high rates of sea level rise. For both models, the value of the critical rate of sea level rise is similar (r_c = 5.2 mm y^{-1}), and spatiality in the Kirwan-model therefore does not influence when the rate-induced critical transition occurs. The erosion factor is only present in the spatial Kirwan-model, so an implication of this would be that erosion on the marsh surface does not have a significant influence on salt marsh stability. Therefore, salt marshes which are prone to erosion factors on the marsh (e.g. a high tidal wave energy) might not be less stable with rising sea level.

To define potential early warning signals for salt marsh collapse in the Morris-model, the eigenvalue of the model close to the rate-induced tipping point has been researched. The eigenvalue has a minimum value for intermediate values of sea level rise and marsh depth, and for high values of biomass productivity (implying the system is most stable under these conditions). Furthermore, if the system has a high biomass productivity, the eigenvalue can both be very negative and close to zero. This implies biomass productivity is not a good predictor of salt marsh stability. In contrast, a high depth of the marsh below mean high tide is a good predictor of the proximity to the critical rate of sea level rise. However, the disadvantage of the salt marsh depth as early warning signal is that it is more difficult to measure in the field, or with remote sensing methods. Therefore, other early warning signals may be more suitable for determining salt marsh stability.

For both the non-spatial and the spatial model, the auto-correlation and the variance were measured for different rates of sea level rise. Both models showed the auto-correlation and the variance increase in proximity to the critical sea level rise value. For the Kirwan-model, this conclusion holds for both the salt marsh surface, the water channel area and the creek cliff. However, the exact values of the early warning signals between the two models differ significantly. The variance on the salt marsh in the Kirwan-model is considerably lower for each rate of sea level rise which is plotted. If early warning signals are measured in the field, it is therefore difficult to determine salt marsh stability with a measurement at one point in time. Instead, it is more insightful to have several measurements of salt marsh stability with different rates of sea level rise, so the relative change in the variance or auto-correlation can be determined.

The salt marsh-specific early warning signals which are researched indicate that both the creek cliff steepness and the marsh surface area decrease towards the tipping point. The decreasing cliff steepness can be explained by the higher marsh depth, causing vegetation is not able to grow on the cliff edge anymore because of a too high inundation pressure. As a consequence, diffusion is higher at the creek cliff edge when sea level rise is higher, so the steepness will decrease. The salt marsh area decreases because the creek cliff moves towards the water divide with a rising sea level. This is caused by the erosion threshold τ_c which is crossed earlier because more water is flowing over the marsh. Both of these early warning signals can help to provide a better overview of salt marsh stability when combined with the measurement of other early warning signals.

Theoretical implications

In this thesis, it is concluded that the presence and/or strength of early warning signals can be different for different parts of the salt marsh. The early warning signals which are studied for the Morris-model all show a smooth increase towards the rate-induced tipping point. However, in the Kirwan-model it is shown that the variance is not uniform for all cells on the salt marsh and can differ several orders of magnitude in the same model run. Therefore, a non-spatial differential equations model can give too generalised results about the stability of an ecosystem, and studying an ecosystem in space can give more elaborate results.

Research limitations

A quantitative research strategy adopted in this thesis, using a mathematical modelling approach. As a consequence, the study has a high internal validity, but a lower external validity. This means that it is difficult to extrapolate the research findings of the study to other models describing salt marsh dynamics or to real world ecosystems. For both models used in this thesis, several assumptions have been made which may not be very realistic. These will now be discussed.

Firstly, both models consider the mean high tide and the saltmarsh height as state variables, but not the biomass productivity. The assumption is that if the salt marsh has the right depth below the mean high tide, the vegetation will grow regardless. However, there could be potential other factors which determine whether vegetation will grow, e.g. the amount of wave energy to which plants are exposed or the amount of erosion. Besides this, to calculate the variance and auto-correlation in a model, the state variable needs to be disturbed to determine how the system will respond to that disturbance. In this model structure, it is not possible to disturb the biomass productivity, because this is not a state variable. Therefore, it cannot be measured how the system would respond to a removal of vegetation.

Secondly, the spatial Kirwan-model does not include scale-dependent feedback, as discussed in the introduction. This is different from the other models describing salt marsh dynamics (see Wesenbeeck et al., 2008), and from models in which spatial warning signals have been identified for arid ecosystems (Rietkerk et al., 2004). Scale-dependent feedback causes erosion around tussocks which form the salt marsh, and therefore could lead to channel formation closer to the water divide as is the case in the current Kirwan-model simulations. This formation of patterns by scale-dependent feedback could lead to early warning signals which may not be present in this study.

Policy implications

Currently, coastal protection focuses mainly on building 'hard' coastal structures which protect the land from rising sea level. However, given that the rate of sea level rise is still increasing, coastal protection infrastructure needs to be continuously checked and fortified (Reed et al., 2018). In this situation, salt marshes can function as soft coastal protection because of their ability to 'keep track' with the rising sea level, thereby protecting the inland. Policy measurements which could increase salt marsh stability are the improvement of sediment influx to the salt marsh and the introduction of plant species which are better able to capture sediment. Besides this, this study showed that close to the rate-induced tipping point, the area of the salt marsh itself can still be resilient against perturbations, even though the total salt marsh area decreases. Having better prediction tools for salt marsh stability can help policy makers to determine what the function of a salt marsh area can be in terms of coastal protection in the future.

Conclusion

In this thesis, several aspects regarding the stability of salt marsh ecosystems have been researched. The first research question was: How do vegetation productivity, suspended sediment concentration and the ability of vegetation to capture sediment affect the stability of salt-marshes subject to sea level rise? A better ability of vegetation to capture sediment and a higher suspended sediment concentration lead to a higher value of sea level rise where the rate-induced critical transition occurs, whereas higher vegetation productivity leads to a lower value of the critical sea level rise. In order to protect salt marshes against rising sea level in the future, a higher sediment supply or plant species better at capturing sediment might therefore be needed.

The second research question was: How do spatial processes affect the critical rate of sea level rise above which sedimentation in salt marsh ecosystems cannot keep up with sea level rise? The Morris-model and the Kirwan-model both have the same value for the critical rate of sea level rise r_c, above which the system does not have biomass productivity and the whole salt marsh area is drowned. This implies that the spatial processes present in the Kirwan-model, i.e. diffusion and creek formation, do not have a significant effect on salt marsh stability.

The third research question was: How can the proximity to a rate-induced critical transition in salt marshes be inferred from statistics on time series and/or spatial patterns? The Morris-model indicates the biomass productivity is not a good predictor of salt marsh stability, because if the system has a high biomass productivity, the eigenvalue of the system can both be very negative and close to zero. Both the Morris-model and the Kirwan-model indicate the auto-correlation and the variance on the salt marsh increase if the rate of sea level rise is close to the tipping point. Salt marsh-specific early warning signals indicate that the creek edge steepness decreases towards the rate-induced tipping point. Furthermore, the percentage of salt marsh area decreases with an increasing rate of sea level rise.

Sources

Bertness, M. D., & Ellison, A. M. (1987). Determinants of pattern in a New England salt marsh plant community. *Ecological Monographs*, *57*(2), 129-147.

Bouma, T. J., Van Belzen, J., Balke, T., Van Dalen, J., Klaassen, P., Hartog, A. M., Callaghan, D. P., Hu, Z., Stive, M. J. F., & Herman, P. M. J. (2016). Short-term mudflat dynamics drive long-term cyclic salt marsh dynamics. *Limnology and oceanography*, *61*(6), 2261-2275.

Heide van der, T., Eklöf, J. S., van Nes, E. H., van der Zee, E. M., Donadi, S., Weerman, E. J., Olff, H., & Eriksson, B. K. (2012). Ecosystem engineering by seagrasses interacts with grazing to shape an intertidal landscape. *PloS one*, *7*(8), e42060.

Kéfi, S., Guttal, V., Brock, W. A., Carpenter, S. R., Ellison, A. M., Livina, V. N., Seekell, D. A., Scheffer, M., van Nes, E. H., & Dakos, V. (2014). Early warning signals of ecological transitions: methods for spatial patterns. *PloS one*, *9*(3), e92097.

Kirwan, M. L., & Guntenspergen, G. R. (2010). Influence of tidal range on the stability of coastal marshland. *Journal of Geophysical Research: Earth Surface*, *115*(F2).

Kirwan, M. L., Guntenspergen, G. R., & Morris, J. T. (2009). Latitudinal trends in Spartina alterniflora productivity and the response of coastal marshes to global change. *Global Change Biology*, *15*(8), 1982-1989.

Kirwan, M. L., & Megonigal, J. P. (2013). Tidal wetland stability in the face of human impacts and sea-level rise. *Nature*, *504*(7478), 53.

Kirwan, M. L., & Murray, A. B. (2007). A coupled geomorphic and ecological model of tidal marsh evolution. *Proceedings of the National Academy of Sciences*, *104*(15), 6118-6122.

Koppel, J. van de., Wal, D. van de, Bakker, J. P., & Herman, P. M. (2005). Self-organization and vegetation collapse in salt marsh ecosystems. *The American Naturalist*, *165*(1), E1-E12.

Liu, Q. X., Doelman, A., Rottschäfer, V., de Jager, M., Herman, P. M., Rietkerk, M., & van de Koppel, J. (2013). Phase separation explains a new class of self-organized spatial patterns in ecological systems. *Proceedings of the National Academy of Sciences*, *110*(29), 11905-11910.

Liu, Q. X., Rietkerk, M., Herman, P. M., Piersma, T., Fryxell, J. M., & van de Koppel, J. (2016). Phase separation driven by density-dependent movement: a novel mechanism for ecological patterns. *Physics of life reviews*, *19*, 107-121.

Maanen van, B., Coco, G., & Bryan, K. R. (2015). On the ecogeomorphological feedbacks that control tidal channel network evolution in a sandy mangrove setting. *Proceedings of the Royal Society A: Mathematical, Physical and Engineering Sciences*, *471*(2180), 20150115.

Meire, P., Ysebaert, T., Van Damme, S., Van den Bergh, E., Maris, T., & Struyf, E. (2005). The Scheldt estuary: a description of a changing ecosystem. *Hydrobiologia*, *540*(1-3), 1-11.

Morris, J. T., Sundareshwar, P. V., Nietch, C. T., Kjerfve, B., & Cahoon, D. R. (2002). Responses of coastal wetlands to rising sea level. *Ecology*, *83*(10), 2869-2877.

Morris, J. T., Sundberg, K., & Hopkinson, C. S. (2013). Salt marsh primary production and its responses to relative sea level and nutrients in estuaries at Plum Island, Massachusetts, and North Inlet, South Carolina, USA. *Oceanography*, *26*(3), 78-84.

Reed, D., van Wesenbeeck, B., Herman, P. M., & Meselhe, E. (2018). Tidal flat-wetland systems as flood defenses: Understanding biogeomorphic controls. *Estuarine, Coastal and Shelf Science*, 213, 269-282.

Rietkerk, M., Boerlijst, M. C., van Langevelde, F., HilleRisLambers, R., van de Koppel, J., Kumar, L., Kumar, L., Prins, H. M. T., & de Roos, A. M. (2002). Self-organization of vegetation in arid ecosystems. *The American Naturalist*, *160*(4), 524-530.

Rietkerk, M., Dekker, S., de Ruiter, P., van de Koppel, J. (2004). Self-Organized Patchiness and Catastrophic Shifts in Ecosystems. *Science*, 305(5692), 1926-1929.

Ritchie, P., & Sieber, J. (2018). Early-warning indicators for rate-induced tipping. *Chaos: An Interdisciplinary Journal of Nonlinear Science*, *26*(9), 93-116.

Rockström, J., Steffen, W., Noone, K., Persson, Å., Chapin III, F. S., Lambin, E. F., Lenton, T. M., Scheffer, M., Folke, C., Schellnbruner, H. J., Nykvist, B., de Wit, C.A., Hughes, T., van der Leeuw, S., Rodhe, H., Sörlin, S., Snyder, P. K., Costanza, R., Svedin, U., Falkenmark, M., Karlberg, L., Corell, R. W., Fabry, V.J., Hansen, J., Walker, B., Liverman, D., Richardson, K., Crutzen, P., & Foley, J. A. (2009). A safe operating space for humanity. *Nature*, *461*(7263), 472-475.

Roman, C. T. (2017). Salt marsh sustainability: challenges during an uncertain future. *Estuaries and coasts*, *40*(3), 711-716.

Scheffer, M., Bascompte, J., Brock, W. A., Brovkin, V., Carpenter, S. R., Dakos, V., Held, H., van Nes, E. H., Rietkerk, M., & Sugihara, G. (2009). Early-warning signals for critical transitions. *Nature*, *461*(7260), 53.

Scheffer, M., Carpenter, S., Foley, J. A., Folke, C., & Walker, B. (2001). Catastrophic shifts in ecosystems. *Nature*, *413*(6856), 591.

Scheffer, M., van Nes, E. H., Holmgren, M., & Hughes, T. (2008). Pulse-driven loss of top-down control: the critical-rate hypothesis. *Ecosystems*, *11*(2), 226-237.

Siteur, K., Eppinga, M. B., Doelman, A., Siero, E., & Rietkerk, M. (2016). Ecosystems off track: rate-induced critical transitions in ecological models. *Oikos*, *125*(12), 1689-1699.

Syvitski, J. P., Vörösmarty, C. J., Kettner, A. J., & Green, P. (2005). Impact of humans on the flux of terrestrial sediment to the global coastal ocean. S*cience*, *308*(5720), 376-380.

Turing, A. M. (1952). The chemical theory of morphogenesis. *Phil. Trans. Roy. Soc*, *13*(1).

Verschuren, P., Doorewaard, H., & Mellion, M. J. (2010). *Designing a research project*. The Hague: Eleven International Publishing.

Wesenbeeck van, B. K., van de Koppel, J., Herman, P. M. J., & Bouma, T. J. (2008). Does scale-dependent feedback explain spatial complexity in salt-marsh ecosystems? *Oikos*, *117*(1), 152-159.

Willemsen, P. W. J. M., Borsje, B. W., Hulscher, S. J. M. H., Van der Wal, D., Zhu, Z., Oteman, B., Evans, B., Möller, I., & Bouma, T. J. (2018). Quantifying bed level change at the transition of tidal flat and salt marsh: can we understand the lateral location of the marsh edge? *Journal of Geophysical Research: Earth Surface*, *123*(10), 2509-2524.

Zedler, J. B., Callaway, J. C., Desmond, J. S., Vivian-Smith, G., Williams, G. D., Sullivan, G., Brewster, A. E., & Bradshaw, B. K. (1999). Californian salt-marsh vegetation: an improved model of spatial pattern. *Ecosystems*, *2*(1), 19-35.

Appendix A: Calculation of the eigenvalue

The stability of salt marsh depth *D* in equation 5 in the *theoretical framework* section for different values of *D* can be determined by determining how a small perturbation *D'* will develop over time.

$$\frac{\mathrm{d}(D+D')}{\mathrm{dt}} = \mathrm{r} - \left(kb(D+D')^3 + ka(D+D')^2 + (qC_{ss}+kc)(D+D')\right)$$

$$= \mathrm{r} - \left(kb(D^3 + 3D^2D' + 3DD'^2 + D'^3) + ka(D^2 + 2DD' + D'^2) + (qC_{ss}+kc)(D+D')\right)$$

$$\approx r - \left(kb(D^3 + 3D^2D') + ka(D^2 + 2DD') + (qC_{ss}+kc)(D+D')\right)$$

$$= r - (kbD^3 + kaD^2 + (qC_{ss}+kc)D + 3kbD^2D' + 2kaDD' + (qC_{ss}+kc)D') \qquad \textit{(A.1)}$$

$$\frac{\mathrm{d}D'}{dt} = \frac{d(D+D')}{dt} - \frac{dD}{dt}$$

$$= \left[r - (kbD^3 + kaD^2 + (qC_{ss}+kc)D + 3kbD^2D' + 2kaDD' + (qC_{ss}+kc)D')\right] - \left[\mathrm{r} - (\mathrm{kb}D^3 + \mathrm{ka}D^2 + (qC_{ss}+kc)\mathrm{D})\right]$$

$$= -(3kbD^2 + 2kaD + qC_{ss} + kc)D \;=\; \lambda D \qquad \textit{(A.2)}$$

with $\lambda = -3kbD^2 - 2kaD - qC_{ss} - kc$. If $\lambda > 0$, then the system will diverge from the steady state and is unstable. If $\lambda = 0$, the system is neutrally stable and the depth *D* will have the value of the critical depth D_c. If $\lambda < 0$, a perturbation in the system will die out and the system will return to its steady state.

Appendix B: Description of the 2-dimensional Kirwan-model

The salt marsh model from Morris et al. (2002) is made spatially explicit by Kirwan and Guntenspergen (2007). In the model, space is modelled by a grid of discrete cells which cover an area of 3 km x 3 km, with the length and width of each cell being 5 m x 5 m. Each cell has two state variables (the salt marsh height *Y2* and the mean high tide *Y3*) which together give the salt marsh depth of each cell ($D = Y3 – Y2$). The model is initialized with a completely subtidal topography slightly sloping towards the right. Five outlet cells are defined at the right edge of the model which are assigned a depth of 500 cm. For each cell, the deposition rate is calculated in the same way as is done in Morris et al. (2002) (see equation 4 in the *theoretical framework* section). The erosion rate and the diffusion are calculated in a slightly different way than the 1-dimensional model, which will now be explained.

To calculate the erosion rate, it is necessary to know the velocity of the water flow over each cell. To calculate the water flow, the direction of the water flow from the water divide to the outlet cell needs to be defined. Firstly, the height of each cell is used to determine whether a cell is part of the salt marsh or part of the channel network. If the cell has a height more than 2 cm beneath the mean marsh height, the cell is considered a channel network cell. Furthermore, all channel network cells need to form a network of cells (via their von Neumann neighbourhood) eventually connected to the outlet cells, otherwise they are still considered part of the marsh (which is necessary to prevent water from streaming into a ‘water pit’).

The second step for determining the erosion rate consists of calculating the direction in which the water flows form the centre of the marsh towards the edges, and into the channel network. The water flow is determined by a water surface which is approximated with a constant curvature Poisson form, implying that the second derivative of the water surface in the horizontal and vertical directions is a constant number. For each cell in the marsh, the water volume will flow towards the adjacent cell in the Moore neighbourhood for which there is the steepest gradient. The map which depicts the flow direction for each cell is called a local drain direction (LDD) map.

Now the actual water velocity in each cell can be calculated. Water will flow through a number of cells until all water has drained to the edge of the marsh. For each cell, the total volume of water which is drained is calculated by multiplying the depth of each cell ($D = Y3 - Y2$) with the length and width of the cell. For each cell, the water volume of all upstream cells is added to its original water volume. This total volume is then used to calculate the flow velocity, which in turn enables the calculation of the erosion rate in each cell (see equation 9 and 10 in the *theoretical framework* section). Together with the deposition rate this leads to a new height for each cell which is used for calculating the diffusion of sediment between cells.

The model has included a diffusion factor for the sediment in order to prevent too large variations in depth between neighbouring cells. This flux is driven by gravitation and occurs in the same direction as the water flow (i.e., the flux direction is given by the LDD map). The diffusion is given by equation 12 in the *theoretical framework* section: The diffusion increases with an increasing slope, whereas the presence of vegetation stabilizes the sediment and therefore decreases the sediment diffusing.

After calculating the diffusion, a new salt marsh height is calculated for every cell. The change in salt marsh height calculated in one time step in the model is multiplied by 120, so one time step represents two months in real time (with each day having two tidal cycles). This new salt marsh height is then used again to calculate the deposition rate, erosion rate and the diffusion.